Surface & Coatings Technology 205 (2010) 1578–1583

Contents lists available at ScienceDirect

Surface & Coatings Technology

journal homepage: www.elsevier.com/locate/surfcoat

Influence of process duration on structure and chemistry of borided low carbon steel

G. Kartal [a], S. Timur [a], O.L. Eryilmaz [b], A. Erdemir [b,*]

[a] Istanbul Technical University, Department of Metallurgical and Materials Engineering, Maslak-Istanbul, Turkey
[b] Argonne National Laboratory, Energy Technology Division, Argonne, IL, USA

ARTICLE INFO

Available online 17 August 2010

Keywords:
Boriding
Electrolysis time
Molten salts
Surface treatment

ABSTRACT

In this study, we employed an ultra-fast boriding technique to grow hard boride layers on low carbon steel substrates using an induction furnace at 900 °C. The technique utilizes an electrochemical cell in which it is possible to achieve very thick (i.e., about 90 μm thick) boride layers in about 30 min. The effects of process duration on boride layer thickness, composition, and structural morphology were investigated using microscopic and X-ray diffraction (XRD) methods. We also developed an empirical equation for the growth rate of boride layers. XRD results revealed two principal boride phases: FeB and Fe_2B thickness of which was very dependent on the process duration. For example, Fe_2B phase was more dominant during shorter boriding times (i.e., up to 15 min.) but FeB became much more pronounced at much longer durations. The growth rate of total boride layer was nearly linear up to 30 min of treatment. However during much longer process duration, the growth rate assumed a somewhat parabolic character that could be expressed as $d = 1.4904\ (t)^{0.5} + 11.712$), where d (in μm) is the growth rate, t (in s) is duration. The mechanical characterization of the borided surfaces in plane and in cross-sections has confirmed hardness values as high 19 GPa at or near the borided surface (where FeB phase is present). However, the hardness gradually decreased to 14 to 16 GPa levels in the region where Fe_2B phase was found.

Published by Elsevier B.V.

1. Introduction

Most of the machine components that are in use today often operate under severe conditions involving adhesive and abrasive wear situations, solid particle erosion, corrosion and oxidation that can substantially degrade their durability and performance. Up to now, a variety of surface engineering and coating techniques have been developed and used to enhance the surface metallurgical and tribological properties of such components [1–3]. The main objective of these techniques has been to increase the mechanical hardness, stiffness, and strength as well as wear and corrosion resistance of such components so that they can last much longer and perform better. Some of the current surface engineering and coating methods involve the creation of a thick and hard case (through the use of conventional nitriding and/or carburizing) followed up by the deposition of a thin hard coating, like CrN or TiC by well-established PVD and/or CVD methods. This is more commonly known as the duplex treatment process and presented extensively in previous literature by Prof. Tom Bell and his coworkers [4,5]. Beside the duplex surface treatments, other methods like flame or induction hardening, laser shot-peening, friction stir-welding, etc. are also available and can be used to produce hard layers on steel and other types of materials [6–10]. In some applications, the deposition of a thin hard coating like TiN, TiAlN, TiC on tool steels could be sufficient to achieve reasonably good resistance to wear and corrosion (due to their high hardness and excellent chemical inertness) [11–13]. However, for most ordinary applications, these coatings may be somewhat expensive and hence not feasible for large volume applications. Instead, the use of conventional thermal diffusion processes like carburizing and nitriding remains as the most preferred option for treating large numbers of parts at very reasonable costs [1–3]. These processes can result in a fairly thick case depth with hardness values ranging from 600 to 1100 Vickers.

Besides the well-adopted nitriding and carburizing processes mentioned above, boriding is another well known thermochemical surface hardening process which can be applied to a wide range of steel components. Unlike these processes, boriding can produce much harder surface layers on ferrous materials with hardness values in the range from 1500 to 2000 HV. Furthermore, boriding can substantially enhance the corrosion, abrasion, and erosion resistance of ferrous materials in nonoxidizing dilute acids and alkali media [14,15].

At present, there are several boriding processes available for the treatment of ferrous materials. The most prominent are pack boriding, paste boriding, liquid or molten salt boriding, electrochemical boriding, plasma boriding, etc. [14,15]. Among others, pack boriding has been used widely by industry, although it suffers from the very long processing time and the generation of huge amounts of solid wastes and gaseous emissions to deal with after the boring treatment. All of the boriding processes mentioned require high processing temperatures (typically in the range of 800–1000 °C) to form the hard iron boride phases either in gaseous, solid or molten salt media [14–

* Corresponding author.
E-mail address: erdemir@anl.gov (A. Erdemir).

0257-8972/$ – see front matter. Published by Elsevier B.V.
doi:10.1016/j.surfcoat.2010.08.050

17]. In general 100 to 150 μm thick boride layers can be formed on plain carbon steels (0.3%C) via pack boriding after 8–10 h of treatment time and at process temperatures of 900 °C and above [18,19].

In this paper, we present the results of a systematic study on electrochemical boriding that is capable of producing very thick boride layers at very fast rates (i.e., about 90 μm in 30 min). The main benefits of this process are much shorter process time, very thick boride layers, and the elimination of the sources of solid or gaseous wastes or emissions (which have become major concerns in recent years) [20,21]. Electrochemical boriding has existed since 1940s and Ornig and Schaaber described the general principles which involved the immersion of cathodically polarized work pieces into molten borax while a graphite bar serving as the anode [14]. Despite these early studies, electrochemical boriding has not attracted much attention and very limited numbers of publications (mostly dealing with the effects of electrolyte composition, current density, and boriding temperature on the structure of resultant boride layers) appeared in open literature [20–30].

The main goal of this study is to more systematically investigate the process and determine the effect of process duration on boride layer morphology, chemistry, thickness, and mechanical properties. Such knowledge could potentially stir more interest in this process and may eventually lead to larger-scale applications as an alternative to conventional boriding processes.

2. Experimental techniques

Low carbon steel substrates (DIN EN 10130-99 DC04, 0.004 Carbon) were cut into small pieces (i.e., 10×40 mm and 2 mm thick) and progressively polished up to 800-grit emery paper to achieve a nominal surface roughness of about 0.1 μm CLA. They were then ultrasonically cleaned in acetone and blow-dried before subjecting to electrochemical boriding treatment. The electrochemical boriding of steel samples was carried out in a high frequency induction furnace containing a graphite crucible acting as an anode and the steel sample acting as a cathode (Fig. 1). The surface area ratio of anode to cathode in the cell is approximately 10. The boriding experiments were carried out in a molten salt that consisted of 90% borax and 10% sodium carbonate at a constant temperature of 900 °C and a current density of 200 mA/cm^2. The constant parameters used in the study are the optimized conditions found in our previous investigations [29,30]. Only the electrolyte supplementary sodium chloride was replaced with sodium carbonate due to this corrosion effect on the electrode connectors. During electrolysis, the temperature of the inner side of electrolyte was controlled by a Pt-PtRh13 thermocouple and the temperature of the outer electrolyte surface was measured periodically by an infrared thermometer.

After completion of the boriding experiment, the current to electrodes was cut off, the steel sample was withdrawn from the electrolyte and left in air to cool down. Frozen remnants of electrolyte on borided sample surface were washed away in boiling water. Cross-sections of the borided samples were progressively ground and polished (SiC papers and 1 μm diamond solution) to reveal the morphology of the boride layers so that they could be observed using an optical microscope. Since boride layers have their unique color or contrast, etching solution was not needed to reveal its morphology. The average thickness of the boride layers at different process durations was determined by measuring the thickness of the layer at eight different locations. The phase composition of boride layer was characterized from the surface of borided samples by thin film X-ray diffraction (XRD) analysis using CuKα radiation (10 kV, 10 mA). Furthermore, the hardness distributions of the cross-sectioned boride

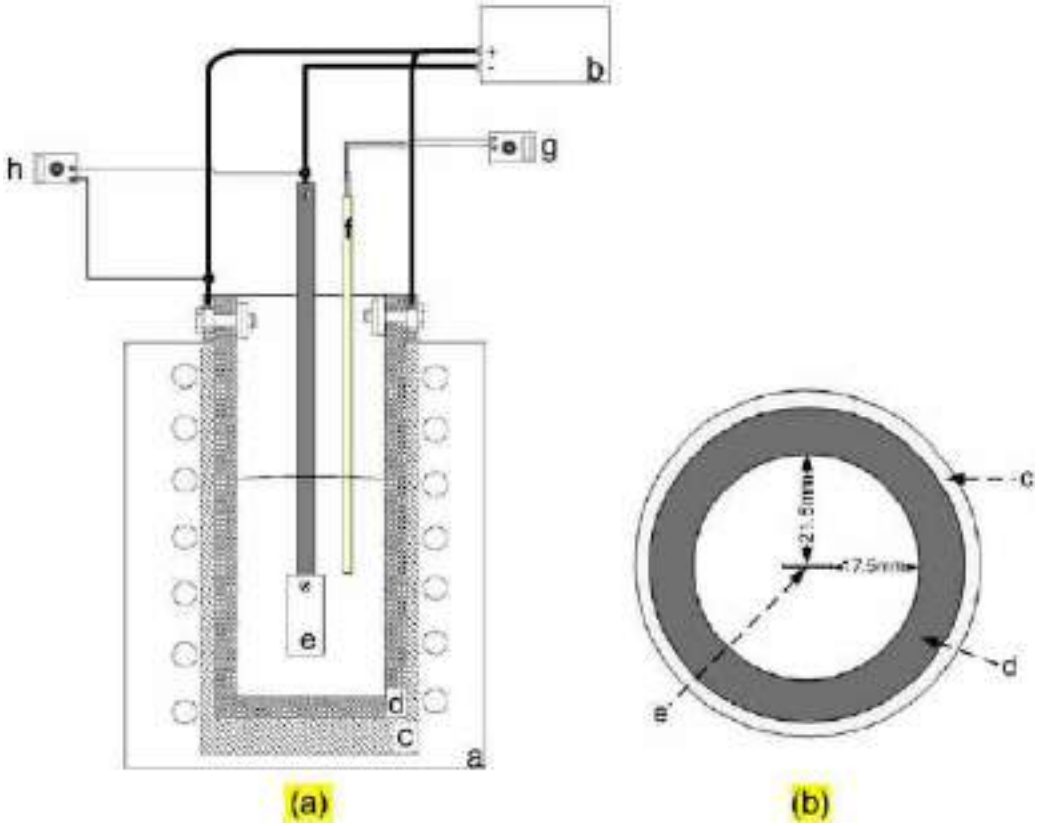

Fig. 1. Schematic drawing of the electrochemical boriding setup, (a) front view (b) top view, a – High frequency furnace, b – Direct current source (±0.001 mA), c – Alumina protector crucible, d – Graphite crucible acting as an anode, e – Cathode f – Thermocouple in alumina protection tube, g – Multimeter (in order to measure temperature), h – Multimeter (in order to measure cell potential).

layers were measured by means of a Vickers microhardness tester with a load of 100gf.

3. Results and discussion

The optical images of the steel samples borided at different time intervals are shown in Fig. 2. As is clear, very dense and homogenously thick boride layers had formed near the surface of the steel substrates (i.e., about 12 μm even after 1 min of electrochemical boriding). The thickness of boride layer increased with increasing processing time. Based on the microscopic images in Fig. 2, it could be deduced that the morphology of the boride layers was more uniform on top and at the interface up to 30 min of boriding; however, it became somewhat ragged or tooth-shaped at the interface after much longer process durations (i.e., 1 h and so). The reason for such tooth-like growth morphology at or near the interface could be due to the preferred diffusion of boron in certain crystallographic orientations like the [001] direction [31,32]. Such an irregular tooth-like growth pattern of boride phase at or near the interface would be very advantageous considering the fact that these would potentially ensure good layer gripping and strong adhesion to the substrate steel. Overall, the boride layers looked very dense and uniform without any evidence of cracks or delamination.

The examination of the thin film XRD analysis of the borided samples (Fig. 3) revealed a stratified boride structure essentially made of Fe_2B (inner) and FeB (outer) phases. Furthermore, the FeB phase became much more dominant as the boride layer became thicker. FeB phase was found near the top surface and we believe that the boron atoms that were available in very large quantities on or near the top were the main reason for iron to react and form FeB (which is the highest boron-containing iron boride phase).

The thickness variations of the FeB and Fe_2B phases as well as the total boride layer are shown in Fig. 4 as a function of process duration. The growth rates of both boride phases was very high during the very first minutes of the electrochemical boriding process; for instance, only after 1 min of boriding 12-μm-thick

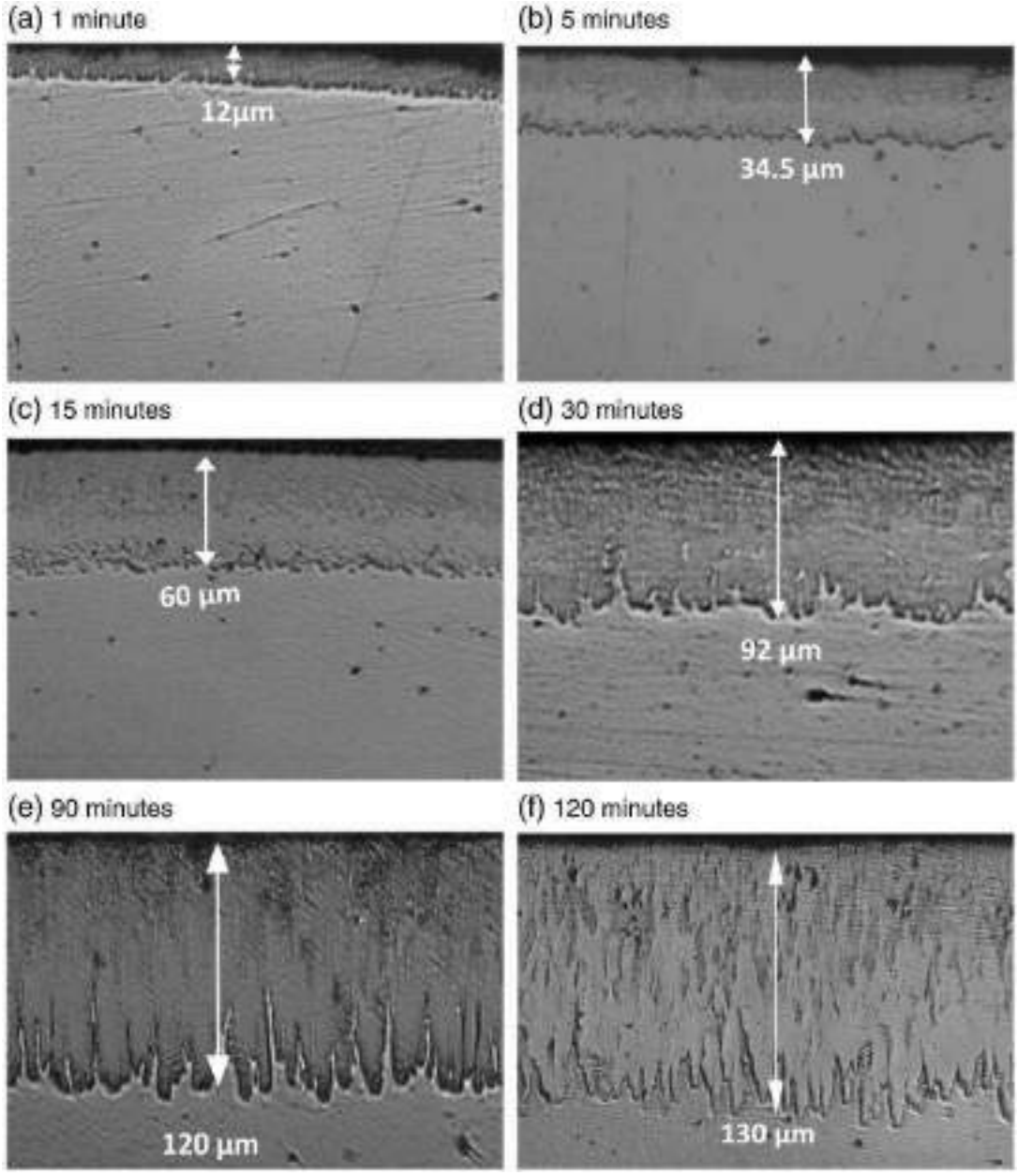

Fig. 2. Cross-sectional optical micrographs of boride layer at different times (×200).

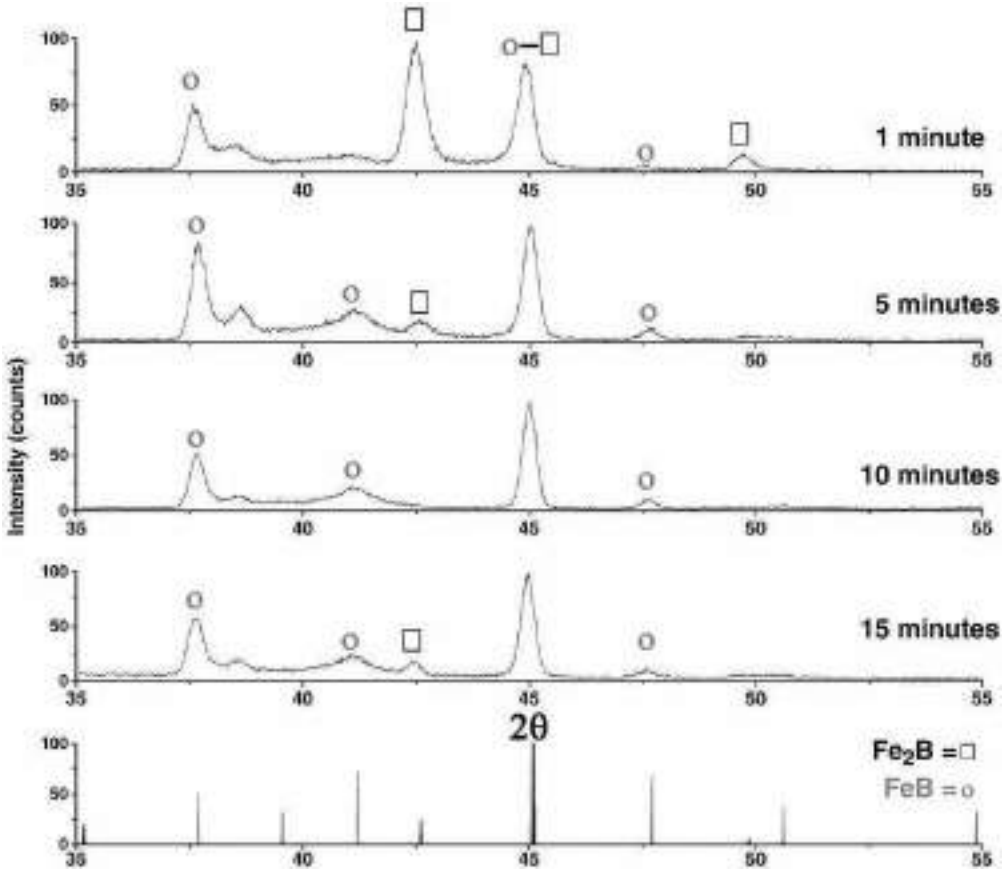

Fig. 3. XRD diffraction pattern of boride layer at different electrolysis times.

Fe_2B boride layer had formed. However this tendency of high speed boride layer formation decreased gradually with time, and about 60 μm thick boride layer (composed of 25 μm FeB and 35 μm Fe_2B phases) was attained in 15 min. In 30 min, more than 90 μm thick boride layer was grown on the steel substrate. Overall, during the first 30 min of the boriding time, there appears to be a linear correlation between the boride layer thickness and process duration. However, beyond this linear growth regime, the rate of boride layer formation showed a tendency to slow down perhaps due to the formation of increasingly thicker boride layer acting as a diffusion barrier as discussed in Ref. 15. Note that the growth behaviors of FeB and Fe_2B are somewhat similar. Up to 30 min of boriding time, they show similar growth patterns; an initially very high growth rate is followed by a reduced growth rate especially after about 60 min of boriding time.

The percentage of individual boride layer (i.e., FeB and Fe_2B) thickness to total boride layer (TBL) thickness with respect to boriding time is shown in Fig. 5. This information is important in terms of revealing the dominant or competitive nature of each phase with respect to the boriding time. During the first 30 min, the contribution of Fe_2B layer on total boride layer decreased considerably; whereas, FeB layer became increasingly more pronounced within the entire boride layer. The reason for this is perhaps due to the fact that the diffusivity of boron at 950 °C is 1.82×10^{-8} cm^2/s for

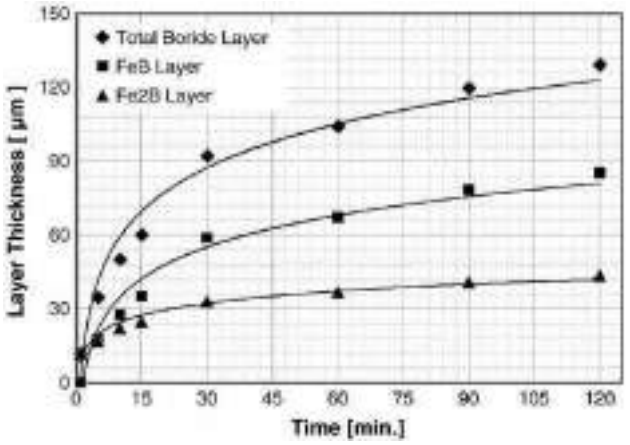

Fig. 4. Variations of boride layers thicknesses (μm) with time (min).

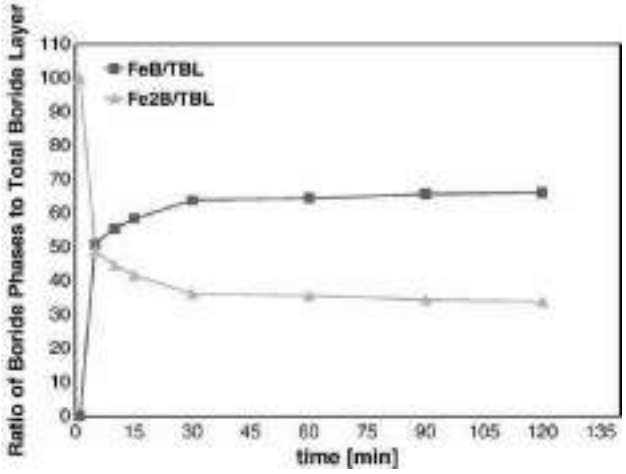

Fig. 5. The ratio of individual boride layer (FeB and Fe_2B) thickness to total boride layer (TBL) thickness as a function of boriding time.

the top boride layer which is 10 times lower than its diffusivity (i.e., 1.53×10^{-7} cm^2/s) within the unborided zone beneath [15]. Therefore after the formation of first Fe_2B layer, its dense structure will undoubtedly slow down the boron diffusion process and thus promote the formation of FeB phase on top. After reaching certain thickness, the growth rate of boride layer will go down again mainly because of the diffusion barrier effect of the top boride layer.

The dependence of the boride layer formation rate on process duration was neither linear nor logarithmic in the long run (see Fig. 4), in fact it had a parabolic character as shown in Fig. 6. This is an expected situation, because boriding is a diffusion-controlled process like other diffusion-controlled carburizing and nitriding processes whose growth rates obey a parabolic law with the simple formula (Eq. (1)) at a given temperature [1,15,21].

$$d^2 = Kt \tag{1}$$

Where d is the case depth, K is the growth rate constant (diffusivity constant) and t is the treatment time. The growth rate constant, K, determines the speed of boride layer formation and depends on the temperature according to Arrhenius equation, the chemical composition of the steel substrate, and the concentration gradient of boron [1,15]. The growth rate constants for total boride layer as well as the FeB and Fe_2B layers were calculated from the slope of straight lines and were found to be 2.223×10^{-12} ms^{-1}, 1.168×10^{-12} ms^{-1}, 0.167×10^{-12} ms^{-1} respectively. FeB layer had greater growth rate constant than Fe_2B layer, in other words the formation of FeB is favored more than Fe_2B phase, especially in the long run. The growth rate constants for boride layers produced by other boriding techniques were included in Table 1. As is clear, electrochemical boriding certainly has higher growth rate values than the other competitive boriding processes, depending on boriding conditions, it is sometimes 27 times faster.

The empirical equations (Eq. (2), Eq. (3), Eq. (4)) inset in Fig. 6 express the change in thickness of all boride layers, d (μm) with respect to the square root of the time of electrolysis ($s^{1/2}$).

$$d_{TBL} = 1.4904(t)^{1/2} + 11.712 \tag{2}$$

$$d_{FeB} = 1.0809(t)^{1/2} + 0.2487 \tag{3}$$

$$d_{Fe2B} = 0.4095(t)^{1/2} + 11.464 \tag{4}$$

Where d_{TBL}, d_{FeB}, d_{Fe2B} are the thickness of total boride layer, thickness of FeB layer and thickness of Fe_2B layer respectively in micrometer and t is the process time in seconds. These equations are

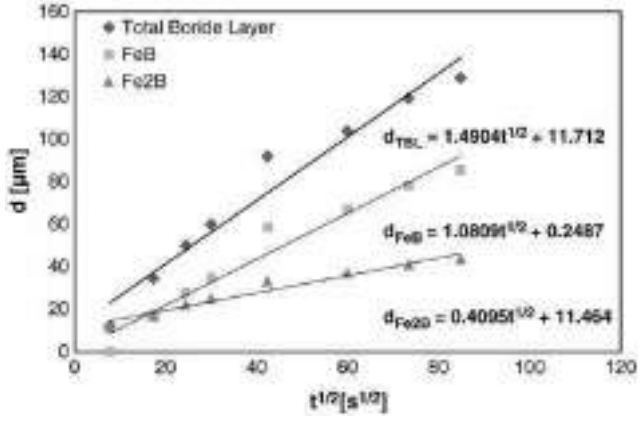

Fig. 6. Dependence of the thickness of boride layers, d_{TBL}, d_{FeB}, d_{Fe2B} on the square root of the time of electrolysis $t^{1/2}$.

Table 1
The growth rate constant values of boride layer produced by other boriding techniques.

Process	Substrate	K, (ms^{-1})	Valid temperature, (K)	Reference
Paste boriding	Armco iron	4.59×10^{-13}	1223	[33]
Paste boriding	AISI 1045	8.26×10^{-14} at 2 mm paste thickness 5.57×10^{-13} at 5 mm paste thickness	1193	[34]

significant to estimate the thickness of boride layer in a given process time and they are valid for the constant electrolyte composition (90% $Na_2B_4O_7$ and 10% Na_2CO_3) and temperature (900 °C) and current density (200 mA/cm^2).

The hardness profile of 1 h electrochemically borided low carbon steel is provided in Fig. 7 in a cross-sectional micrograph. The hardness of the borided layer showed a tendency to decrease as we moved from top to interior. Since the contrast difference between the dominant boride layers (i.e., FeB and Fe_2B) were clearly distinguishable in the micrograph, the top part of boride layer with a darker contrast was FeB layer with the composition of 16.23 wt.% (or 50 at.%) boron and the lighter secondary (inner) boride layer was Fe_2B phase with the composition of 8.83 wt.% (or 33 at.%) boron [14,15]. The variation of hardness could be divided into three distinct regions; FeB dominant area with hardness values of 1900 to 1600 HV, Fe_2B region with hardness values of 1600 to 1000 HV, and transition zone in which the hardness value was higher than the matrix hardness with the range of 600 to 250 HV. Apparently, the electrochemical boriding

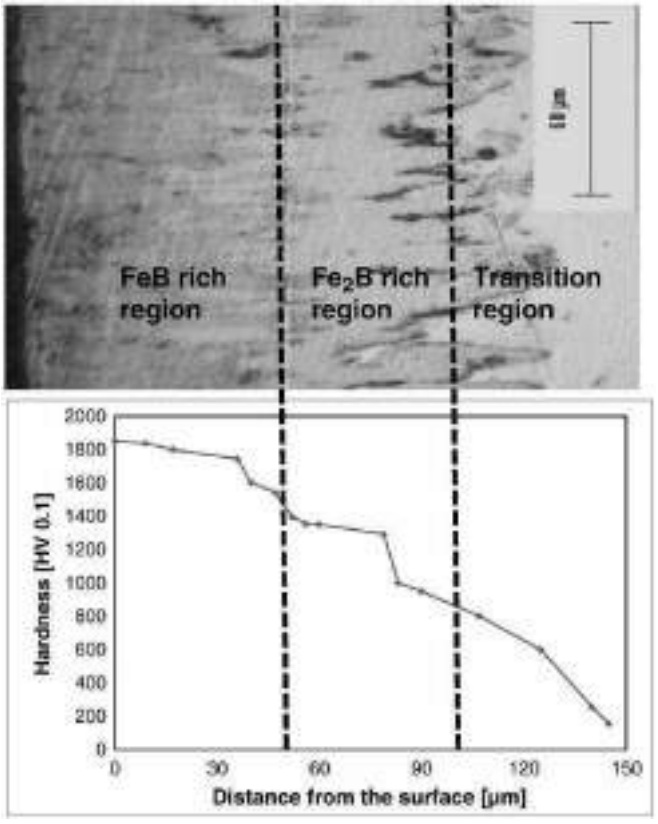

Fig. 7. Typical cross-sectional optical micrograph of 1 h borided steel and corresponding hardness profile.

is able to increase the hardness (i.e., 150 HV) of low carbon steel by more than an order of magnitude, especially toward the top surface.

Based on the results presented, we can state that the production of hard and thick iron borides is feasible with the electrochemical boriding technique. Based on their very impressive hardness values, such boride layers could potentially be very useful for applications that require high resistance to abrasive and erosive wear (detailed studies are currently underway and will be published separately). Overall, electrochemical boriding may be considered as an alternative to traditional boriding techniques (like pack-boriding, paste boriding, salt-bath boriding, plasma boriding) all of which suffer from slow boriding rates, emissions and waste problems, as well as high cost.

4. Conclusion

- Very dense and homogenously thick boride layers could be formed on low carbon steel substrates during very short processing time in electrochemical boriding. The morphology of boride layers is very uniform at the interface for the first 30 min of boriding time; however, it tends to become more finger-like with longer process durations (1 h and so).
- Within the first 30 min of processing time, more than 90 μm thick boride layers were produced at 900 °C in an electrolyte consisting of 90% borax and 10% sodium carbonate and at a current density of 200 mA/cm^2.
- Electrochemically borided layers consisted of a stratified structure made of Fe_2B (inner) and FeB (outer). FeB phase became more dominant boride phase with increasing electrolysis time.
- The growth rate constant for electrochemical boriding was as high as 2.223×10^{-12} ms^{-1} at 900 °C which is 5 to 27 times higher than the conventional boriding processes.
- The dependence of the rate of the boride layer formation on process duration had a parabolic character. Specifically, the growth rate of boride layer could be represented by the equation:

$$d_{\mathrm{TBL}} = 1,4904\,(t)^{0.5} + 11.712$$

where d (in μm) is the growth rate, t (in s) is duration of electrolysis;

The hardness of borided layer varied between 1000 (near the interface) and 1900 HV (near the top).

References

[1] S. Lampman, ASM Handbook: Heat Treating: Surface Hardening of Steels, 4, 1991.
[2] G. Kraus, J Heat Treat 9 (1992) 81.
[3] R.S. Petrova, N. Suwattananont, J Electron Mater 34 (2005) 575 No5.
[4] Y. Sun, T. Bell, Trans Inst Met Finish 70 (1992) 38.
[5] K. Mao, Y. Sun, A. Bloyce, T. Bell, Surf Eng 26 (2010) 142.
[6] Z.Y. Ma, Metall. Mater. Trans. (2008) 642 39A.
[7] M.K. Lee, G.H. Kim, K.H. Kim, W.W. Kim, Surf. Coat. Technol. 184 (2004) 239.
[8] A. Bokota, S. Iskierka, Int. J. Mech. Sci 40 (1998) 617.
[9] P. Peyre, X. Scherpereel, L. Berthe, C. Carboni, R. Fabbro, G. Beranger, C. Lemaitre, Mater Sci Eng A 280 (2000) 294.
[10] R.S. Mishra, Z.Y. Ma, Mater Sci Eng (2005) 1 R50.
[11] W. Tillmann, E. Vogli, S. Momeni, Vacuum 84 (2010) 387.
[12] N.J.M. Carvalho, A.J.H. Veld, J. De Hosson, Surf. Coat. Technol. 105 (1998) 109.
[13] C.Y.H. Lim, S.C. Lim, K.S. Lee, Wear (1999) 225 354.
[14] A.G. Von Matuschka, Boronizing, Heyden and Son Inc, 1980.
[15] A.K. Sinha, Boriding, 4, 1990.
[16] T.W. Spence, M.M. Makhlouf, J Mater Process Technol 168 (2005) 127.
[17] O. Ozdemir, M.A. Omar, M. Usta, S. Zeytin, C. Bindal, A.H. Ucısık, Vacuum 83 (2009) 175.
[18] C. Bindal, A.H. Ucisik, Vacuum 82 (2008) 90.
[19] V. Jain, G. Sundararajan, Surf Coat Technol 149 (2002) 21.
[20] L. Segers, A. Fontana, R. Winand, Electrochim Acta 36 (1991) 41.
[21] K. Matiasovsky, M. Chrenkova-Paucirova, P. Fellner, M. Makyta, Surf Coating Technol 35 (1988) 133.
[22] S.H. Han, J.S. Chun, J Mater Sci 15 (1980) 1379.
[23] P. Gopalakrishnan, P. Shankar, M. Palaniappa, S.S. Ramakrishnan, Metall Mater Trans A (2002) 1475 33A.
[24] M. Makyta, K. Matiasovsky, P. Fellner, Electrochim Acta 29 (1984) 1653.
[25] B.V. Badushkin, B.Z. Polyakov, Met Sci Heat Treatment 15 (1973) 577.
[26] V.N. Tkachev, P.K. Grigorov, B.B. Katkhanov, Met Sci Heat Treatment 17 (1975) 348.
[27] G. Kaptay, S.A. Kuznetsov, Plasmas Ions 2 (1999) 45.
[28] M. Makyta, M. Chrenkova, P. Fellner, K. Matiasovsky, Z Anorg Allg Chem 540 (1986) 169.
[29] G. Kartal, O. Kahvecioglu, S. Timur, Surf Coat Technol 200 (2006) 3590.
[30] G. Kartal, S. Timur, C. Arslan, J Electron Mater 34 (2005) 1538.
[31] E. Melkndez, I. Campos, E. Rocha, M.A. Barron, Mater Sci Eng A (1997) 900.
[32] A.J. Ninham, I.M. Hutchings, J. Vac. Sci. Technol. (1986) 2827 A4.
[33] J. Campos, U. Oseguera, J.A. Figueroa, O. Garcia, Bautista, G. Kelemenis, Mater Sci Eng (2003) 261 A352.
[34] O. Campos, G. Bautista, M. Ramirez, J. De La Parra, L. Zuniga, Appl Surf Sci 243 (2005) 426.